Rho protein regulates tight junctions and perijunctional actin organization in polarized epithelia

A. NUSRAT*, M. GIRY†, J. R. TURNER*, S. P. COLGAN‡, C. A. PARKOS*, D. CARNES*, E. LEMICHEZ†, P. BOQUET†, AND J. L. MADARA*

Departments of *Pathology and ‡Anesthesia, Division of Gastrointestinal Pathology, Brigham and Women's Hospital and Harvard Medical School, Boston, MA 02115; and †Unite des Toxines Microbiennes, Institute Pasteur, 75724 Paris, France

ABSTRACT The rho family of GTP-binding proteins regulates actin filament organization. In unpolarized mammalian cells, rho proteins regulate the assembly of actin-containing stress fibers at the cell–matrix interface. Polarized epithelial cells, in contrast, are tall and cylindrical with well developed intercellular tight junctions that permit them to behave as biologic barriers. We report that rho regulates filamentous actin organization preferentially in the apical pole of polarized intestinal epithelial cells and, in so doing, influences the organization and permeability of the associated apical tight junctions. Thus, barrier function, which is an essential characteristic of columnar epithelia, is regulated by rho.

The rho proteins are members of a large family of small GTP-binding proteins (21 kDa) that are believed to be involved in regulating assembly of the actin cytoskeleton. In unpolarized mammalian cells, rho proteins (rhoA, B, and C) regulate assembly of focal adhesions and basal filamentous (F) actin stress fibers (1). The *Clostridium botulinum* toxin C3 transferase selectively blocks rho–effector coupling by ADP-ribosylation of rho on Asn-41 (2–4) and has been a useful tool in examining the biological function of rho proteins. In fibroblasts, C3 transferase induces disassembly of stress fibers that are localized at the base of cells (3, 5). Conversely, microinjection of a constitutively activated form of rho into quiescent serum-starved cells results in the appearance of prominent stress fibers and focal adhesions at the cell–matrix interface (1, 6).

Polarized columnar epithelial cells, such as those lining the alimentary tract, airways, and renal tubules, differ markedly from spreading unpolarized cells in which rho biology has largely been studied. For example, intestinal epithelial cells maintain a tall cylindrical form, have apical intercellular tight junctions that serve as barriers to restrict paracellular permeability, and exhibit morphologically defined subdomains of cytoskeletal structure. Stable lateral and basal F-actin filaments form a submembrane cortex thought to assist in maintaining the cylindrical shape of columnar epithelial cells and in anchoring a variety of basolateral membrane proteins. In contrast, the apical pole of polarized epithelial cells consists of a perijunctional tensile ring of F-actin and myosin II, thought to influence tight junction permeability, and an ordered array of F-actin bundles that stabilize the complex structure of the apical membrane (7–9).

Our aim in the present study was to determine the role of rho in regulating actin cytoskeletal organization in polarized epithelia. Our approach was to study the effects of blocking its functions by uncoupling it from downstream effectors with the C3 transferase exoenzyme in a polarized human intestinal cell line, T84 (10). T84 cells grown on permeable supports form confluent monolayers of columnar epithelia that have apical

and basolateral membranes, high transepithelial resistance to passive ion flow, and a Cl⁻ secretory pathway analogous to that found in native intestinal crypt epithelium. We have also determined the effects of rhoC overexpression in intestinal epithelial cell lines. Our data indicate that rho plays an important regulatory role in determining microfilament organization in the apical pole of columnar epithelial cells and, in so doing, influences the associated tight junction and epithelial permeability. Concurrent with these effects, ZO-1, a tight junction structural element, moves off the membrane, while E-cadherin, the sealing element of the closely related adherens junction, is preserved on the membrane.

MATERIALS AND METHODS

Cell Culture and Electrophysiology. T84 cells (ATCC) and Caco-2BBE (Mark Mooseker, Yale University) were passaged and grown on collagen-coated permeable supports as described (8). Measurement of transepithelial resistance and flux of fluoresceinated dextran was performed by using standard biophysical techniques (8).

In Vitro **Ribosylation Assay.** T84 cells were grown as polarized monolayers with high transepithelial electrical resistance (>1000 ohm·cm²) on 5-cm² permeable supports. Experimental monolayers were exposed to the chimeric toxin DC3B (1.6 μg/ml) for 70 hr in serum-free medium while control monolayers were identically treated in the absence of DC3B. *In vitro* ribosylation assay was performed as described (11). Briefly the ADP-ribosylation reaction was performed by incubating 1% of the postnuclear supernatant with a mixture containing [³²P]NAD (5 × 10⁵ cpm) and recombinant C3 exoenzyme (4 μg/ml). The reactions were stopped by adding sample buffer. SDS/PAGE was performed; the gel was dried and autoradiographed on x-ray film.

Immunofluorescence. Confluent monolayers of the human intestinal epithelial cell line T84 were grown on collagen-coated permeable supports as described (12) and exposed to DC3B (0.5–1.6 μg/ml) or serum-free medium. Cells were washed in Hanks' balanced salt solution, fixed in methanol (for E-cadherin) or 3.7% (wt/vol) paraformaldehyde (for ZO-1 and actin), permeabilized in acetone (for ZO-1 and actin), stained first with a monoclonal antibody to E-cadherin or polyclonal antibody to ZO-1 (Zymed) and subsequently with fluoresceinated secondary antibodies. To identify actin microfilaments, cells were incubated with rhodamine phalloidin for 40 min. Monolayers mounted in PBS/glycerol/*p*-phenylenediamine, 1:1:0.01 (vol/vol), were analyzed by confocal microscopy.

Transfection. pKC vesicular stomatis virus glycoprotein-tagged rhoC was isolated from bacteria by using a Qiagen column (Chatsworth, CA). Isolated DNA was used to transfect subconfluent colonies of cells by using Lipofectin (Life Technologies, Gaithersburg, MD). After 72 hr, cells were fixed in paraformaldehyde, permeabilized in acetone, and stained with antibody to the vesicular stomatitis virus tag of rhoC, followed
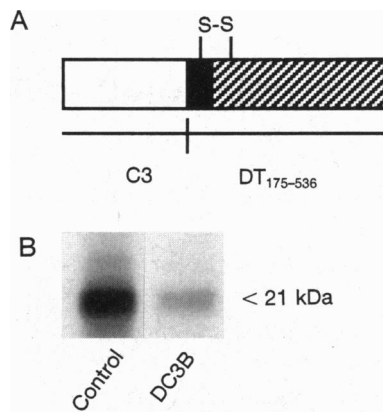
FIG. 1. DC3B mediates ADP-ribosylation of rho in polarized T84 intestinal epithelial monolayers. (*A*) The DC3B chimera consists of the entire C3 transferase fused to the C terminus (residues 175–536) of diphtheria toxin, which conserves the first disulfide loop domain for translocation and the receptor binding domain (11). (*B*) *In vitro* C3 transferase-mediated ADP-ribosylation of rho in cell lysates obtained from control or DC3B-preexposed T84 cells. DC3B preexposure largely inhibits subsequent ribosylation of rho in lysates indicating its effectiveness in ribosylating rho in intact cells. Scanning of this gel revealed a density of 505 OD units for control and 151 OD units for DC3B-exposed cells.

by a fluorescein isothiocyanate-conjugated secondary antibody and rhodamine phalloidin. Transfected cells expressing the epitope-tagged rhoC in the center of colonies were selected for examination since such areas provide polarized epithelial cells (in contrast to cells at the edge of colonies).

Immunoprecipitation and Western Blot Analysis. E-cadherin and ZO-1 immunoprecipitation, SDS/PAGE, and Western blot analysis were performed as described (13, 14).

RESULTS AND DISCUSSION

C3 transferase exoenzyme was used to determine the effects of ADP-ribosylation of rho on the structure and function of model polarized intestinal epithelia composed of T84 cells (8). To ensure widespread and efficient translocation of C3 exoenzyme into monolayers of polarized epithelial cells grown on permeable supports, we utilized a chimeric toxin, DC3B. The C3 gene was fused to DNA encoding diphtheria toxin modified to ablate toxin activity but preserve the cell-binding B domain (11) (Fig. 1*A*). Rho in intact T84 intestinal epithelial cells is efficiently ADP-ribosylated by the chimeric toxin at concentrations and durations of exposure identical to those required for its ADP-ribosylation in unpolarized eukaryotic cells (Fig. 1*B*). DC3B-mediated ADP-ribosylation of rho resulted in marked selective effects on cytoskeletal F-actin (Fig. 2). While
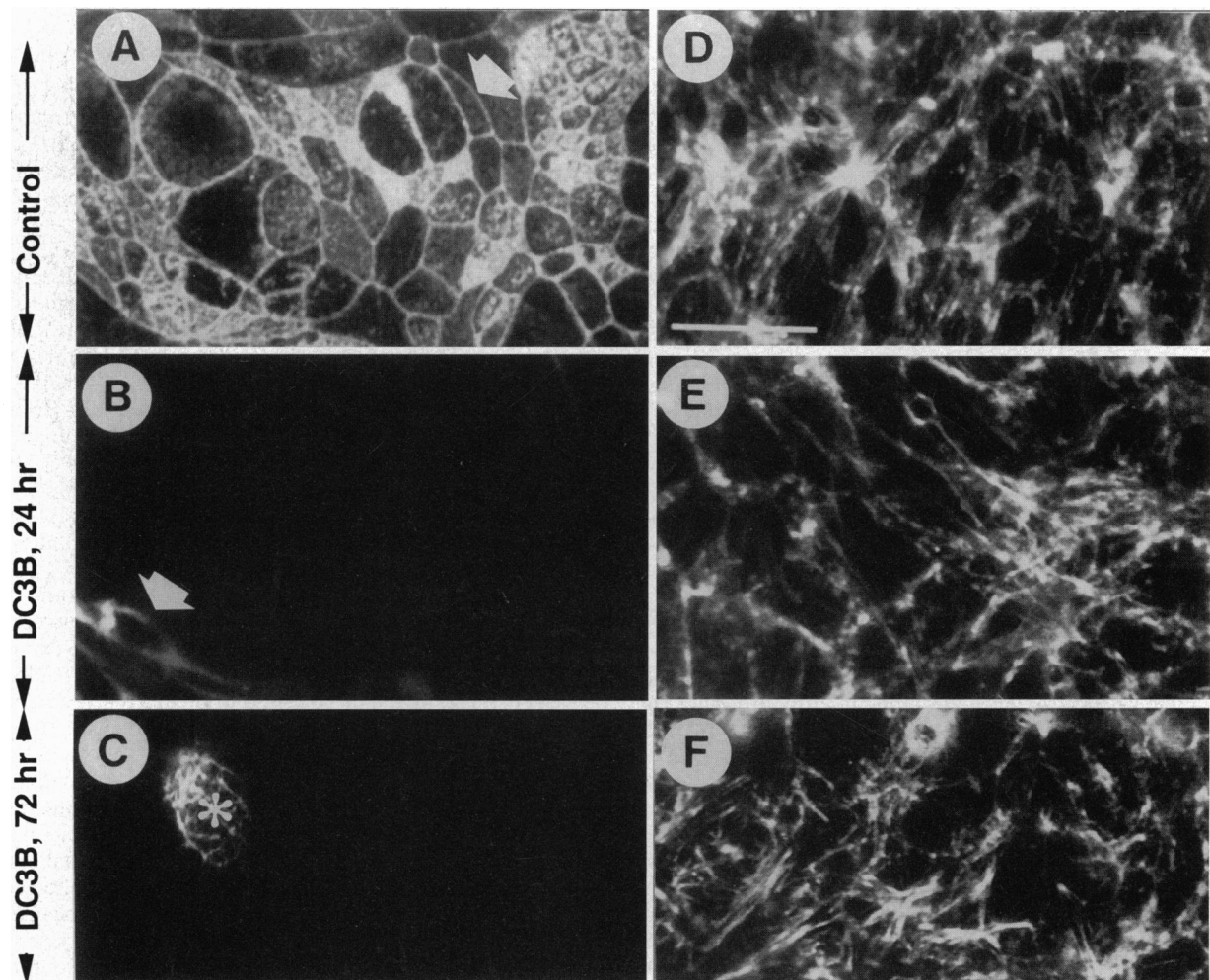

FIG. 2. F-actin distribution in control (serum-free medium) or DC3B-exposed monolayers for 0, 24, or 72 hr. Confocal microscopic localization of F-actin in *en face* optical sections taken at the apical (*A–C*) or basal (*D–F*) planes of monolayers are shown. Normally, F-actin in the apical plane of the monolayer (*A*) is densely arrayed in perijunctional rings and as fine stippling that represents microvillus actin bundles. After DC3B exposure, apical F-actin is confined to occasional patchy areas at 24 hr (*B*) (arrow) and is lost in all but rare cells by 72 hr (*C*) (asterisk, indicating the only cell in the broad low-magnification field in which apical actin staining could be detected). In contrast, F-actin in the basal stress fibers (*D–F*) does not appear to be affected by DC3B. (All images are at a uniform magnification. Bar in *D* ≈ 40 μm.)

F-actin of the basal stress fibers (Fig. 2 *D–F*) was not noticeably changed by ADP-ribosylation of rho, F-actin in the apex of the cell including the perijunctional ring was disassembled (Fig. 2 *A–C*). Subjunctional lateral cortical F-actin also appeared unaffected after ADP-ribosylation of rho (data not shown). Comparable findings were obtained in the unrelated polarized intestinal epithelial cell line Caco-2$_{BBE}$ (15). This selective effect on apical and perijunctional F-actin organization is remarkably similar to that described after exposure of intestinal epithelia to *Clostridium difficile* toxin A—a causative agent associated with the human disease pseudomembranous colitis (16). Emerging evidence suggests that *C. difficile* toxin A elicits chemical modifications of rho that may be central to its action, although the specific modification appears not to be ADP-ribosylation (17). The alterations in monolayer function mediated by ribosylation of rho were not accompanied by a loss of membrane integrity of individual cells (as shown by measurements of the release of soluble intracellular proteins such as lactate dehydrogenase; data not shown).

To further define the role of rho as a regulator of perijunctional actin organization, polarized intestinal epithelial cells were transiently transfected with epitope-tagged rhoC (18). Cells transfected with rhoC displayed thickening of F-actin bundles throughout the cell, at the level of the apical perijunctional ring, the lateral cortex, and the basal stress fibers (Fig. 3). In contrast, mock-transfected cells or cells transiently overexpressing cytoskeletal elements such as villin do not display such diffusely thickened F-actin bundles.

Given that the perijunctional F-actin ring is a potential regulator of tight junction permeability and is thus integral to defining characteristics of columnar epithelial barrier function (19), the effects of DC3B-mediated ADP-ribosylation of rho on epithelial permeability were assessed. Measurements of transepithelial resistance to passive ion flow and tight junction permeability to 10-kDa dextran indicate that tight junction permeability was markedly increased by DC3B under conditions in which no detectable cytotoxicity (morphology or lactate dehydrogenase release) occurred and cells maintained intimate contact and columnar shape (Fig. 4 *G* and *H*). Comparable effects on tight junction permeability have also been reported for *C. difficile* toxin A of pseudomembranous colitis that targets rho function. The DC3B enzyme exerted its effects only when applied to the basolateral compartment (data not shown), consistent with the known basolateral distribution of diphtheria toxin B subunit receptor in polarized epithelial cells (20).

Given that ADP-ribosylation of rho appears to elicit dramatic but relatively selective alterations in apical actin and the associated tight junction, the distribution of two proteins thought to be crucial to organization of the junctional complex was assessed. Distribution of E-cadherin was determined since E-cadherin-based homeotypic adhesive interactions that occur on the lateral membrane just below the tight junction are believed to represent proximal signals in the cascade of events that culminate in the formation and maintenance of tight junctions (21–24). The distribution of E-cadherin on the lateral membrane was not affected by ADP-ribosylation of rho (Fig. 4). Total immunoprecipitable E-cadherin was likewise unaffected by ADP-ribosylation of rho.

In contrast to the membrane localization of E-cadherin, the tight-junction-specific peripheral membrane protein ZO-1 was displaced from the membrane at sites of tight junctions after ADP-ribosylation of rho. This was likely due to dispersion of ZO-1 to the cytoplasm, rather than degradation of ZO-1, as total cellular ZO-1, determined by immunoprecipitation, was unaffected (Fig. 4). ZO-1, a member of the dlg protein family that serves regulatory roles at cytosol–membrane interfaces (25), intimately associates with apical F-actin microfilaments, and coprecipitates with other tight-junction-specific proteins that are further removed from the cytosolic face of the
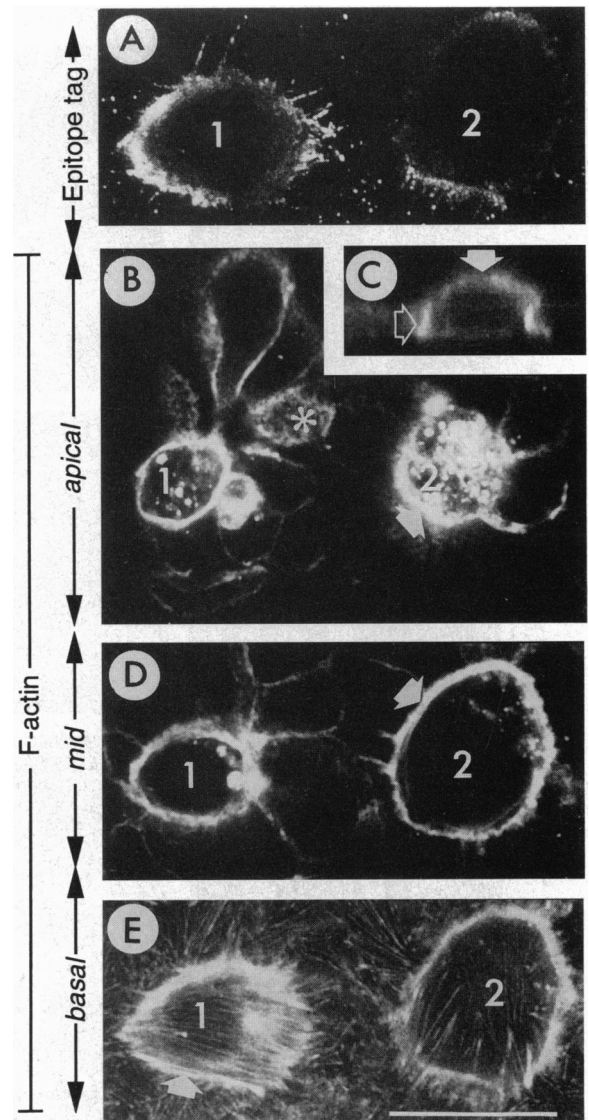

FIG. 3. Overexpression of epitope-tagged rhoC and F-actin organization in polarized epithelial cells. (*A*) Identification (by staining with antibodies to the epitope tag) of two transfected cells (cells 1 and 2) surrounded by nontransfected cells. This represents an *en face* image of the epitope-tagged rho in the basal region of these transfected cells. (*B*) *En face* view of F-actin at the apical surface of the monolayer. The perijunctional rings of the two transfected cells (cells 1 and 2, arrow) are dense in comparison to neighboring nonexpressing cells (asterisk). Thick F-actin aggregates are located in the apical region of transfected cells 1 and 2. (*C*) Transverse *x–z* image of one of the transfected cells demonstrates a slightly rounded apical surface (solid arrow) and dense cortical F-actin (open arrow). (*D*) *En face* view in the middle region of cells showing dense cortical F-actin in the transfected cells (arrow). (*E*) Basal F-actin stress fibers in the two rhoC-overexpressing cells (cells 1 and 2) are focally and modestly thickened (arrow) but cortical F-actin remains strikingly prominent at this site. The adjacent nontransfected cells serve as controls. (Bar = ≈10 μm.)

membrane. For these reasons, it is likely that ZO-1 plays a role in transducing cytoskeletal signals that regulate tight-junction permeability. Time-course studies of rho-ribosylation-associated effects on perijunctional ring F-actin loss, ZO-1 displacement, and enhanced tight junction permeability indicated that these three events appeared to occur synchronously rather than sequentially (data not shown).

These data indicate that rho plays a regulatory role in determining the cytoskeletal organization in the apical pole of columnar epithelial cells, particularly the perijunctional F-
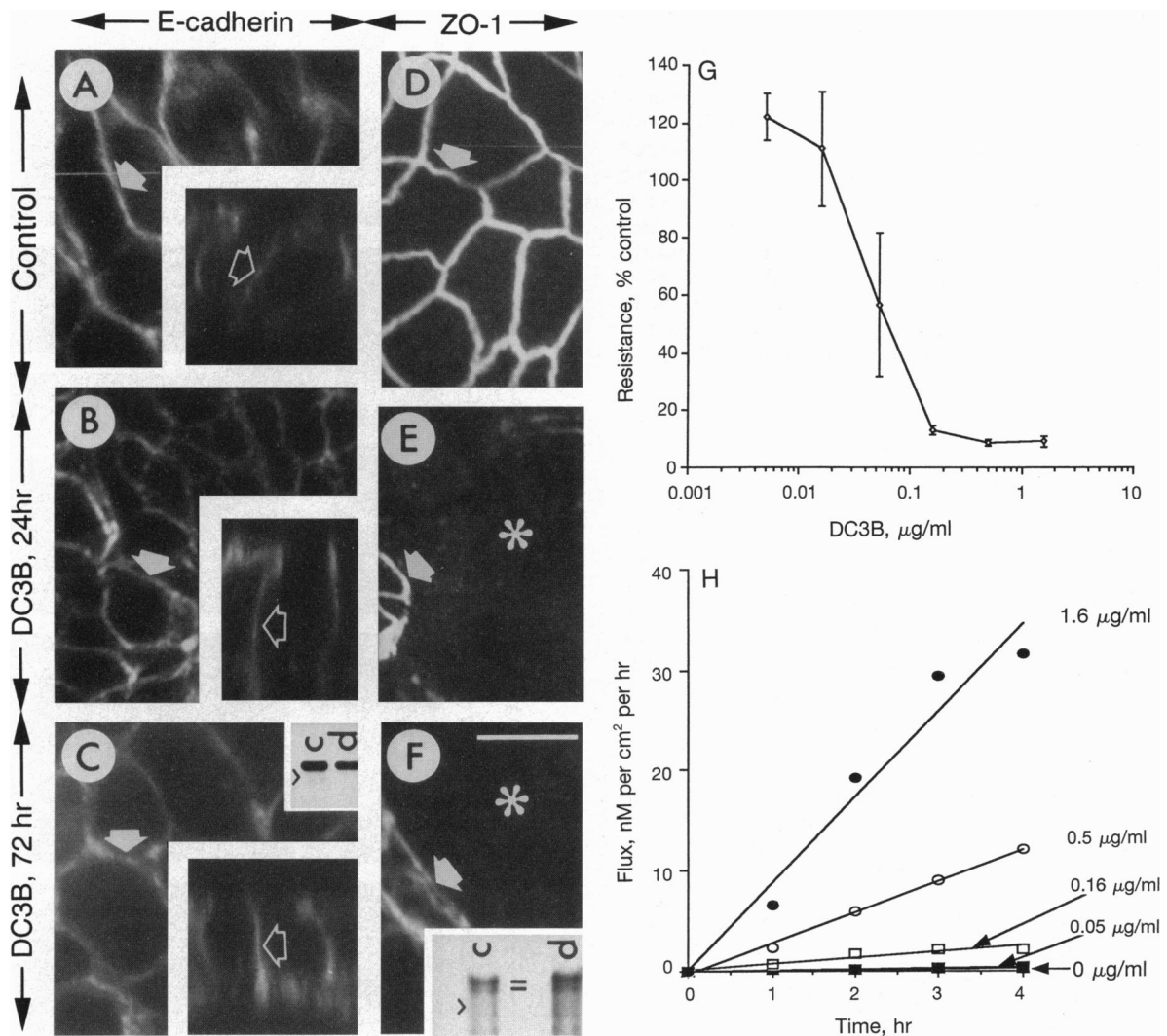
FIG. 4. Distribution of the intercellular adhesive protein E-cadherin in polarized epithelial cells that were not exposed to DC3B (*A*) or exposed to DC3B for 24 (*B*) or 72 hr (*C*). E-cadherin localization in the lateral membrane (arrow) of control cells is not influenced by DC3B exposure. (*Insets Lower Right*) The x–z images displaying uniform distribution of E-cadherin along the lateral membranes (arrow). (*C*) (*Inset Upper Right*) Immunoprecipitable E-cadherin was also unaffected by DC3B exposure. Data represent one of three experiments. >, 116-kDa marker; c, control; d, DC3B. (*D–F*) Distribution of ZO-1 in the plane of the intercellular tight junction in monolayers not exposed (*D*) or exposed to DC3B for 24 (*E*) or 72 (*F*) hr. Linear perijunctional arrangement of ZO-1 (*D*) (arrow) is largely lost after ribosylation of rho mediated by DC3B (asterisks in *E* and *F*)—only occasional islands (*E*) (arrow) or rare individual cells (*F*) (arrow) with perijunctional ZO-1 distribution remain. (*F Inset*) Total cellular ZO-1, as determined by immunoprecipitation, does not change after DC3B exposure, suggesting that ZO-1 is not degraded but has moved off its perijunctional membrane site. Data represent one of three experiments. >, 206-kDa marker; =, position of two closely migrating ZO-1 isoforms; c, control; d, DC3B. (*G* and *H*) Functional characteristics of epithelial monolayers conferred by DC3B-mediated ribosylation of rho (24-hr exposure). (*G*) DC3B lowers the transepithelial resistance to passive ion flow in epithelial monolayers in a dose-dependent fashion with maximal response at 0.5 µg/ml. (*H*) The cumulative transmonolayer flux of an inert hydrophilic solute (10-kDa dextran) is increased in a dose-dependent manner after DC3B exposure. The x axis of *H* refers to the time interval after initiation of measurement of transepithelial flux of fluoresceinated dextran. DC3B-mediated ribosylation of rho, therefore, alters the permeability of intercellular tight junctions that are structurally associated with the perijunctional actin ring.

actin ring. In so doing, rho may exert regulatory influence on the distribution of the tight-junction-specific protein ZO-1 without influencing the membrane distribution of E-cadherin. Such regulatory influences on cytoskeletal architecture and ZO-1 localization appear to have direct functional consequences on tight-junction permeability and, consequently, on epithelial barrier function. These observations strongly suggest that rho may play a pivotal role in regulation of this crucial physiologic event in polarized columnar epithelia.

1. Ridley, A. J. & Hall, A. (1992) *Cell* **70,** 389–399.
2. Aktories, K., Braun, S., Rosener, S., Just, I. & Hall, A. (1989) *Biochem. Biophys. Res. Commun.* **158,** 209–213.
3. Chardin, P., Boquet, P., Maduale, P., Popoff, M. R., Rubin, E. J. & Gill, D. M. (1989) *EMBO J.* **8,** 1087–1092.
4. Sekine, F., Fujiwara, M. & Narumiya, S. (1989) *J. Biol. Chem.* **264,** 8602–8605.
5. Rubin, E. J., Gill, D. M., Boquet, P. & Popoff, M. R. (1988) *Mol. Cell. Biol.* **8,** 418–426.
6. Paterson, H. F., Self, A. J., Garrett, M. D., Just, I., Aktories, K. & Hall, A. (1990) *J. Cell Biol.* **111,** 1001–1007.
7. Mooseker, M. S. (1985) *Annu. Rev. Cell Biol.* **1,** 209–241.

8. Madara, J. L. & Dharmsathaphorn, K. (1985) *J. Cell Biol.* **101,** 2124–2133.
9. Madara, J. L. (1992) *Cell* **53,** 497–498.
10. Madara, J. L., Stafford, J., Dharmsathaphorn, K. & Carlson, S. (1987) *Gastroenterology* **92,** 1133–1145.
11. Aullo, P., Giry, M., Olsnes, S., Popoff, M. R., Kocks, C. & Boquet, P. (1993) *EMBO J.* **12,** 921–931.
12. Shapiro, M., Matthews, J., Hecht, G., Delp, C. & Madara, J. L. (1991) *J. Clin. Invest.* **87,** 1903–1909.
13. Jesaitis, L. A. & Goodenough, D. A. (1994) *J. Cell Biol.* **124,** 949–961.
14. Nusrat, A., Parkos, C., Bacarra, A., Godowski, P., Delp-Archer, C., Rosen, E. & Madara, J. (1994) *J. Clin. Invest.* **93,** 2056–2065.
15. Peterson, M. D. & Mooseker, M. S. (1992) *J. Cell Sci.* **102,** 581–600.
16. Hecht, G., Pothoulakis, C., Lamont, J. T. & Madara, J. L. (1988) *J. Clin. Invest.* **56,** 1053–1061.
17. Just, I., Selzer, J., Eichel-Streiber, C. & Aktories, K. (1995) *J. Clin. Invest.* **95,** 1026–1031.
18. Adamson, P., Paterson, H. F. & Hall, A. (1992) *J. Cell Biol.* **119,** 617–627.
19. Gumbiner, B. M. (1993) *J. Cell Biol.* **123,** 1631–1633.
20. Melby, E. L., Jacobsen, J., Olsnes, S. & Sandvig, K. (1993) *Cancer Res.* **53,** 1755–1760.
21. Behrens, J., Mareel, M. M., Van Roy, F. M. & Birchmeier, W. (1989) *J. Cell Biol.* **108,** 2435–2447.
22. Takeichi, M. (1987) *Trends Genet.* **3,** 213–217.
23. Takeichi, M. (1990) *Annu. Rev. Biochem.* **59,** 237–252.
24. Gumbiner, B., Stevenson, B. & Grimaldi, A. (1988) *J. Cell Biol.* **107,** 1575–1587.
25. Willott, E., Balda, M. S., Fanning, A. S., Jameson, B., Van Itallie, C. & Anderson, J. M. (1993) *Proc. Natl. Acad. Sci. USA* **90,** 7834–7838.